

# Fermi-hypernetted-chain study of unprojected wave functions to describe the half-filled state of the fractional quantum Hall effect

O. Ciftja

*Ames Laboratory and Department of Physics and Astronomy, Iowa State University, Ames, Iowa 50011  
and International School for Advanced Studies, Via Beirut 2-4, I-34014, Trieste, Italy*

S. Fantoni

*International School for Advanced Studies, Via Beirut 2-4, I-34014, Trieste, Italy  
and International Centre for Theoretical Physics, P.O. Box 586, I-34014, Trieste, Italy*

(Received 4 December 1997; revised manuscript received 7 May 1998)

The Fermi hypernetted-chain theory is applied to study the half-filled state of the fractional quantum Hall effect in the thermodynamic limit. We study in detail the radial distribution function, the correlation energy, and the quasiparticle-quasihole excitation spectrum of an unprojected Fermi wave function of the form  $\psi_{\nu=1/2}^{Fermi} = \prod_{j<k}^N (z_j - z_k)^2 \text{Det}\{\phi_{\vec{k}}(\vec{r})\}$ , a possible candidate to describe the half-filled state. Adopting a technique originating from nuclear physics, we compute the effective mass of the fermion excitations near the Fermi surface for this wave function. We find it to be exactly the bare mass of the electron, in accordance with the mean field approximation of not imposing the lowest Landau level constraint. Similar calculations were performed on other related wave functions, which, based on the composite fermion picture, describe the half-filled state of the electrons as a limit of infinite-filled composite fermion Landau levels. [S0163-1829(98)01736-6]

## I. INTRODUCTION

The fractional quantum Hall effect<sup>1</sup> (FQHE) results from a strongly correlated incompressible liquid state<sup>2</sup> formed at special uniform densities  $\rho_e$  of a two-dimensional (2D) electronic system, subject to a strong transverse magnetic field  $\vec{B}$ . For a completely spin-polarized (spinless) system of electrons the dominant sequence of fractional Hall states occurs for filling factors of the lowest Landau level (LLL)  $\nu = p/(2p + 1)$ , where  $p \neq 0$  is an integer.

The first step in the FQHE explanation would be the study of the properties of a 2D fully spin-polarized (spinless) system of  $N$  interacting electrons emerging in a uniform positive background, with the magnetic field  $\vec{B}$  high and temperature  $T$  low, such that only the LLL would be partially filled.

At  $T=0$ , the interaction energies  $\sim \nu^{1/2} (1/4\pi\epsilon_0) \times (e^2/\epsilon l_0)$ , where  $l_0 = \sqrt{\hbar/eB}$  is the magnetic length and  $\epsilon$  is the dielectric constant of the background, are weak compared to the Landau level splitting  $\hbar\omega_c$ , and so all electrons are considered to remain in the LLL. Electrons with charge  $-e$  ( $e > 0$ ) are considered as usual to be confined in the  $x$ - $y$  plane, subjected to the magnetic field  $\vec{B} = [0, 0, B]$  generated from the symmetric gauge vector potential  $\vec{A}(\vec{r}) = [-(B/2)y, (B/2)x, 0]$ . The many-electron system is described by the Hamiltonian

$$\hat{H} = \hat{K} + \hat{V}, \tag{1}$$

with

$$\hat{K} = \frac{1}{2m_e} \sum_{j=1}^N [-i\hbar\vec{\nabla}_j + e\vec{A}(r_j)]^2 \tag{2}$$

and

$$\hat{V} = \sum_{j<k}^N v(|\vec{r}_j - \vec{r}_k|) - \rho_e \sum_{j=1}^N \int d^2r v(|\vec{r}_j - \vec{r}|) + \frac{\rho_e^2}{2} \int d^2r_1 \int d^2r_2 v(|\vec{r}_1 - \vec{r}_2|), \tag{3}$$

where  $m_e$  is the electron's mass,  $z_j = x_j + iy_j$  is the location of the  $j$ th electron in complex coordinates,  $v(|\vec{r}_j - \vec{r}_k|) = (1/4\pi\epsilon_0)(e^2/\epsilon|z_j - z_k|)$  is the interaction potential, and  $\hat{V}$  contains the electron-electron, electron-background, and background-background interaction potential.

From a theoretical point of view, the occurrence of Hall plateaus at filling factors of the form  $\nu = 1/m$ ,  $m = 1, 3, 5$ , can be understood through the original ideas of Laughlin,<sup>3</sup> which described these states by a trial many-electron wave function of the Jastrow type:

$$\psi_m = \prod_{j<k}^N (z_j - z_k)^m \prod_{j=1}^N \exp\left(-\frac{|z_j|^2}{4l_0^2}\right). \tag{4}$$

By construction, this wave function lies entirely in the LLL and describes a translationally invariant isotropic and incompressible liquid of electrons at a density  $\rho_e = \nu/2\pi l_0^2$ , corresponding to the LLL filling factor  $\nu = 1/m$ , where  $m = 1, 3, \dots$ . In contrast, the behavior of such a system in the vicinity of a filling factor with an even denominator, such as  $\nu = 1/2$ , is not well understood. A Laughlin-like Bose wave function  $\psi_{\nu=1/2}^{Bose} = \prod_{j<k}^N (z_j - z_k)^2 \prod_{j=1}^N \exp(-|z_j|^2/4l_0^2)$  does not correctly describe such a situation and a different theory is needed for such fillings.

The paper is organized as follows. Section II presents a brief summary of the Chern-Simons (CS) theory at half filling. Section III presents a brief summary of the Fermi hypernetted-chain (FHNC) approach and its extension to treat different correlated wave functions of the Fermi type. The method to compute the excitation spectrum near the Fermi surface is described in Sec. IV. Numerical results are presented and discussed in Sec. V. Sec. VI is devoted to the conclusions.

## II. CHERN-SIMONS TRANSFORMATION

At  $\nu=1/2$  the typical features of the FQHE, that is, the quantized  $\sigma_{xy}=\nu(e^2/h)$  and vanishing  $\sigma_{xx}$ , are not observed, but nevertheless this state shows a broad minimum<sup>4</sup> in  $\rho_{xx}$  and exhibits, additionally, anomalous behavior in surface acoustic wave propagation,<sup>5</sup> indicating a different type of correlation. Numerical work by Haldane<sup>6</sup> suggested that  $\nu=1/2$  is not incompressible.

Recently a theory of a compressible Fermi-liquid-like behavior at  $\nu=1/2$  was proposed by Halperin, Lee, and Read.<sup>7</sup> According to this theory, a 2D system of electrons subjected to an external perpendicular magnetic field  $\vec{B}$ , with a LLL filling factor  $1/2$ , can be transformed to a mathematically equivalent system of fermions interacting with a Chern-Simons gauge field such that the average effective magnetic field acting on the fermions is zero.

Let me mention some fundamental properties of this transformation, supposing that  $|\Phi(z_1 \cdots z_N)\rangle$  is a solution of the Schrödinger equation  $\hat{H}\Phi = E\Phi$ . Then, for an even number  $q_e$ , where  $q_e=2,4,\dots$ , the wave function

$$\Psi(z_1 \cdots z_N) = \prod_{i < j}^N \frac{(z_i - z_j)^{q_e}}{|z_i - z_j|^{q_e}} |\Phi(z_1 \cdots z_N)\rangle \quad (5)$$

is a solution to the Schrödinger equation  $\hat{H}'\Psi = E\Psi$ , with

$$\hat{H}' = \hat{K}' + \hat{V} \quad (6)$$

and

$$\hat{K}' = \frac{1}{2m_e} \sum_{j=1}^N \{-i\hbar \vec{\nabla}_j + e[\vec{A}(r_j) - \vec{a}(r_j)]\}^2, \quad (7)$$

where  $\vec{a}(\vec{r})$  is the Chern-Simons vector potential

$$\vec{a}(\vec{r}) = \frac{q_e}{2\pi} \phi_0 \sum_{j=1}^N \frac{\vec{z} \times (\vec{r} - \vec{r}_j)}{|\vec{r} - \vec{r}_j|^2} \quad (8)$$

and  $\phi_0$  is the magnetic field flux quantum. The Chern-Simons magnetic field  $\vec{b}(\vec{r})$  associated with the vector potential  $\vec{a}(\vec{r})$  is given by

$$\vec{b}(\vec{r}) = \vec{\nabla} \times \vec{a}(\vec{r}) = q_e \phi_0 \sum_{j=1}^N \delta(\vec{r} - \vec{r}_j) = \rho(\vec{r}) q_e \phi_0, \quad (9)$$

where  $\rho(\vec{r})$  is the local particle density. In other words, the Chern-Simons transformation can be described as the exact modeling of an electron as a fermion attached to  $q_e$  flux

quanta. Assuming a uniform density, the Chern-Simons flux quanta attached to the fermions are smeared out in a uniform magnetic field of magnitude

$$\langle \vec{b} \rangle = \rho_e q_e \phi_0, \quad (10)$$

with  $\rho_e$  the average electronic density.

At special filling factors  $\nu = \phi_0 \rho_e / B = 1/q_e$ ,  $q_e = 2, 4, \dots$ , the applied magnetic field precisely cancels the Chern-Simons flux, so at the mean field level the system can be described as fermions in a zero magnetic field and should therefore be a compressible Fermi-looking liquid state. When  $\nu$  is away from  $1/q_e$ , the applied magnetic field and the Chern-Simons one do not cancel, so a residual effective field

$$B^* = B - q_e \phi_0 \rho_e = B(1 - q_e \nu) \quad (11)$$

is left over. Thus the mean field system is described as non-interacting fermions in a uniform field  $B^*$ . The effective filling factor for these gauge transformed fermions  $p = \rho_e \phi_0 / B^*$  is  $1, 2, \dots$ , corresponding to the integer quantum Hall effect of these gauge transformed fermions.

The ‘‘true’’ filling factor of the electrons  $\nu = \rho_e \phi_0 / B$  is just  $\nu = (p/q_e p + 1)$ , which is precisely the composite fermion (CF) Jain series<sup>8</sup> of FQHE states. The excitation gaps for these quantized Hall states are naturally given by the corresponding effective cyclotron frequency of the CF's:

$$E_g = \hbar \omega_c^* = \hbar \frac{eB^*}{m_{gap}^*(\nu)}, \quad (12)$$

where  $m_{gap}^*(\nu)$  is the effective mass.

In the following we concentrate on the filling  $\nu=1/2$ , where several related wave functions have been employed to incorporate the physics of CF's on it. They can be treated as the limit of the series  $\nu = p/(2p+1)$  for  $p \rightarrow \infty$  and may have different origins. The wave function

$$\Psi_{\nu=1/2}^{CS}(B^*) = \lim_{p \rightarrow \infty} \hat{P}_{LLL} \prod_{j < k}^N \frac{(z_j - z_k)^2}{|z_j - z_k|^2} |\Phi_p(B^*)\rangle \quad (13)$$

appears as the mean field solution of the CS theory,<sup>9</sup> while

$$\Psi_{\nu=1/2}^{CF}(B) = \lim_{p \rightarrow \infty} \hat{P}_{LLL} \prod_{j < k}^N (z_j - z_k)^2 |\Phi_p(B)\rangle \quad (14)$$

is due to the CF theory of Jain. In the above expressions,  $\hat{P}_{LLL}$  is the LLL projection operator and  $|\Phi_p(B)\rangle$  is the Slater determinant wave function of  $p$  filled Landau levels, evaluated at the magnetic field shown in the argument. These two wave functions have different origins and different short-distance behavior in the radial distribution function, but they both describe CF's at half filling since there are two vortices bound to each electron. From the CS theory, we know that at exactly  $\nu=1/2$  the fermions ‘‘see’’ no net magnetic field, so they can form a Fermi sea, which does have a uniform density. As a consequence we would expect that the half-filled state should be well described by a Fermi many-electron wave function of the form

$$\Psi_{\nu=1/2}^{Fermi} = \hat{P}_{LLL} \prod_{j < k}^N (z_j - z_k)^2 \text{Det}\{\varphi_{\vec{k}}(\vec{r})\}, \quad (15)$$

where  $\varphi_{\vec{k}}(\vec{r})$  are normalized plane waves in two dimensions.

In order to have the correct density of the half-filled case, the Fermi surface of the fully spin polarized electrons must have the radius  $k_F = 1/l_0$ . Excited states involve the creation of quasiparticle-quasihole pairs near this Fermi-like surface and these excitations should have an effective mass  $m^*(k)$  determined by interelectron interactions only. The interaction energy per particle  $u(\nu) = (1/N)(\langle \Psi_\nu | \hat{V} | \Psi_\nu \rangle / \langle \Psi_\nu | \Psi_\nu \rangle)$  is computed for the unprojected wave function  $\Psi_{\nu=1/2}^{Fermi}$  and is compared with the respective values for the other unprojected wave functions  $\Psi_{\nu=1/2}^{CS}$  and  $\Psi_{\nu=1/2}^{CF}(B)$ , taken as the limit of infinite filled Landau levels.

In this paper we employ the FHNC formalism to study in detail the unprojected Fermi half-filled wave function  $\Psi_{\nu=1/2}^{Fermi}$ . Within this formalism we incorporate a scheme to study the resulting Fermi excitations near the Fermi surface and we compute the resulting effective mass of such excitations.

### III. THE FERMI HYPERNETTED-CHAIN FORMALISM FOR THE HALF-FILLED FERMI WAVE FUNCTION

The FHNC theory is very useful to perform calculations in the thermodynamic limit for infinite systems of particles interacting via central, spin-independent potentials, with Hamiltonian of the form of Eq. (1). If such systems are described by trial functions of the Jastrow-Slater form, as is the case, then the FHNC theory is applicable. A Jastrow-Slater trial wave function can quite generally be written as

$$|\Psi\rangle = \prod_{i < j}^N f(|\vec{r}_i - \vec{r}_j|) |\Phi\rangle, \quad (16)$$

where a possible choice for  $|\Phi\rangle$  is a Slater determinant making  $|\Psi\rangle$  antisymmetric.

Let us show in some detail the quantities entering the calculation of the  $\Psi_{\nu=1/2}^{Fermi}$  wave function, which contains a determinant of 2D normalized plane waves. The same technique is used to perform similar calculations on  $\Psi_{\nu=1/2}^{CS}$  and  $\Psi_{\nu=1/2}^{CF}(B)$  wave functions, so we skip a detailed description of them. In order to calculate the interaction energy per particle  $(1/N)(\langle \Psi_\nu | \hat{V} | \Psi_\nu \rangle / \langle \Psi_\nu | \Psi_\nu \rangle)$  and the ‘‘kinetic’’ energy per particle  $(1/N)(\langle \Psi_\nu | \hat{K} | \Psi_\nu \rangle / \langle \Psi_\nu | \Psi_\nu \rangle)$ , we should find the radial distribution function  $g(|\vec{r}_i - \vec{r}_j|)$  through the application of the FHNC.

Because of the ‘‘healing’’ property of the factor  $f^2(r_{ij}) - 1 = h(r_{ij}) \rightarrow 0$  as  $r_{ij} \rightarrow \infty$  the spatial correlations present in the wave function may be ordered in powers of the function  $h(r_{ij})$ ,

$$|\Psi|^2 = \left[ 1 + \sum_{i < j}^N h(r_{ij}) + \sum_{i < j}^N \sum_{k < l}^N h(r_{ij})h(r_{kl}) + \dots \right] |\Phi|^2. \quad (17)$$

The (reduced) single-particle density matrix for the dynamically uncorrelated state is given by

$$\hat{\rho}(\vec{r}_1, \vec{r}_2) = g_s \sum_{|\vec{k}| \leq k_F} n(\vec{k}) \varphi_{\vec{k}}^*(\vec{r}_1) \varphi_{\vec{k}}(\vec{r}_2), \quad (18)$$

where the ground state occupation number for a fully spin polarized (spinless) 2D ideal Fermi gas ( $g_s = 1$ ) is

$$n(\vec{k}) = \begin{cases} 1, & |\vec{k}| \leq k_F \\ 0, & |\vec{k}| > k_F. \end{cases} \quad (19)$$

The normalized single-particle states of a 2D gas of free electrons occupying an area  $A$  are  $\varphi_{\vec{k}}(\vec{r}) = (1/\sqrt{A}) e^{i\vec{k} \cdot \vec{r}}$  and  $k_F = 1/l_0$ . A trivial calculation of the statistical exchange factor  $l(\vec{r}_1, \vec{r}_2) = \hat{\rho}(\vec{r}_1, \vec{r}_2)/\rho$  gives

$$l(\vec{r}_1, \vec{r}_2) = 2 \frac{J_1(k_F r_{12})}{k_F r_{12}}, \quad (20)$$

where  $r_{12} = |\vec{r}_2 - \vec{r}_1|$  and  $J_1(x)$  is the first-order Bessel function.

Within the permutation expansion method of Fantoni and Rosati,<sup>10</sup>  $|\Phi|^2$  may be expanded in the number of permutations of particles or the number of exchange factors. After insertion into the expansion (17) the product may be ordered according to the number of particles involved. The resulting cluster terms contain both kinds of correlations and may be represented by cluster diagrams. As in the Bose case, the associated radial distribution function  $g(r)$  is then given by the sum of all linked irreducible diagrams obeying well-defined topological rules.<sup>10</sup>

One defines *nodal*, *non-nodal* (composite), and *elementary* diagrams as in the Bose case, but there are now four different types for each of them. The four different classes of nodal and elementary diagrams are generally denoted by *dd* (direct-direct), *de* (direct-exchange), *ee* (exchange-exchange), and *cc* (circular-exchange). The sums of non-nodal (composite) diagrams of the four types are given by

$$X_{dd}(r_{12}) = f^2(r_{12}) e^{N_{dd}(r_{12}) + E_{dd}(r_{12})} - N_{dd}(r_{12}) - 1, \quad (21)$$

$$X_{de}(r_{12}) = f^2(r_{12}) e^{N_{dd}(r_{12}) + E_{dd}(r_{12})} \times [N_{de}(r_{12}) + E_{de}(r_{12})] - N_{de}(r_{12}), \quad (22)$$

$$X_{ee}(r_{12}) = f^2(r_{12}) e^{N_{dd}(r_{12}) + E_{dd}(r_{12})} [N_{ee}(r_{12}) + E_{ee}(r_{12}) + |N_{de}(r_{12}) + E_{de}(r_{12})|^2 - g_s |N_{cc}(r_{12}) + E_{cc}(r_{12}) - l(r_{12})/g_s|^2] - N_{ee}(r_{12}), \quad (23)$$

$$X_{cc}(r_{12}) = f^2(r_{12}) e^{N_{dd}(r_{12}) + E_{dd}(r_{12})} [N_{cc}(r_{12}) + E_{cc}(r_{12}) - l(r_{12})/g_s] + l(r_{12})/g_s - N_{cc}(r_{12}). \quad (24)$$

The radial distribution function is composed of the components

$$g(r_{12}) = 1 + X_{dd}(r_{12}) + N_{dd}(r_{12}) + 2[X_{de}(r_{12}) + N_{de}(r_{12})] + X_{ee}(r_{12}) + N_{ee}(r_{12}). \quad (25)$$

The chain formation of the nodal diagrams is generated by convolution equations

$$N_{dd}(r_{12}) = \rho \int d\vec{r}_3 [X_{dd}(r_{13}) + N_{dd}(r_{13})] P(r_{32}), \quad (26)$$

$$N_{de}(r_{12}) = \rho \int d\vec{r}_3 [X_{dd}(r_{13})X_{ee}(r_{32}) - X_{de}(r_{13})X_{de}(r_{32}) + [X_{de}(r_{13}) + N_{de}(r_{13})]P(r_{32})], \quad (27)$$

$$N_{ee}(r_{12}) = \rho \int d\vec{r}_3 [X_{de}(r_{13})X_{de}(r_{32}) - X_{dd}(r_{13})X_{ee}(r_{32}) + [X_{ee}(r_{13}) + N_{ee}(r_{13})]P(r_{32})], \quad (28)$$

$$N_{cc}(r_{12}) = \rho \int d\vec{r}_3 [-l(r_{13})/g_s + X_{cc}(r_{13}) + N_{cc}(r_{13})]X_{cc}(r_{32}), \quad (29)$$

with

$$P(r_{ij}) = X_{dd}(r_{ij}) + 2X_{de}(r_{ij}) + \rho \int d\vec{r}_k \times [X_{dd}(r_{ik})X_{ee}(r_{kj}) - X_{de}(r_{ik})X_{de}(r_{kj})]. \quad (30)$$

The FHNC relations provide a closed set of equations for the nodal and non-nodal components appearing in Eqs. (21)–(24) and (26)–(29) only, if the elementary contributions (described by elementary diagrams) are known. Several different approximation schemes are available for an appropriate evaluation of the elementary portions. However, at present we neglect such diagrams adopting the so-called FHNC/0 approximation, where the 0 means neglect of elementary diagrams. In this approximation we set  $E_{\alpha,\beta} = 0$ , where the indices are  $(\alpha,\beta) = (dd), (de), (ee),$  and  $(cc)$ .

For convenience, we substitute  $f(|\vec{r}_i - \vec{r}_j|)^2 = e^{U(|\vec{r}_i - \vec{r}_j|)}$  in the expression of  $|\Psi|^2$  and then we separate the pseudopotential associated with the Jastrow part  $U(r_{12}) = 4 \ln(|z_1 - z_2|)$  into a short- and a long-ranged part, respectively,

$$U_s(r_{12}) = -4K_0(Qr_{12}), \quad (31)$$

$$U_l(r_{12}) = 4K_0(Qr_{12}) + 4 \ln(r_{12}). \quad (32)$$

The function  $K_0(x)$  is the standard modified Bessel function and the wave number  $Q$  is a cutoff parameter of order  $1/l_0$ . Furthermore, all nodal and non-nodal functions are separated into their respective short- and long-range parts and the FHNC/0 equations are solved by a standard iterative procedure.

#### IV. THE PARTICLE-HOLE EXCITATION SPECTRUM OF THE FERMI HALF-FILLED STATE

In this section we report a method to compute the quasiparticle-quasihole Fermi excitations for the Fermi wave function  $\Psi_{\nu=1/2}^{Fermi}$ . For a correlated 2D Fermi gas calculations of the ground state energy  $E_0$  are generally carried out with the wave function

$$\Psi_0 = \hat{C}\Phi(n(\vec{k})), \quad (33)$$

where  $\hat{C}$  is a correlation operator and  $\Phi(n(\vec{k}))$  is a 2D Fermi gas wave function with occupations  $n(\vec{k})$ . Let us compute the energies of a quasiparticle/quasihole state obtained with wave functions  $\Psi_p(\vec{p})$  for  $|\vec{p}| > k_F$  and  $\Psi_h(\vec{q})$  for  $|\vec{q}| < k_F$ :

$$\Psi_p(\vec{p}) = \hat{C}\Phi(n(\vec{k}) + \delta_{p,\vec{k}}^-), \quad (34)$$

$$\Psi_h(\vec{q}) = \hat{C}\Phi(n(\vec{k}) - \delta_{q,\vec{k}}^-), \quad (35)$$

Let  $E_p(p)$  and  $E_h(q)$  be the energies obtained with these wave functions. The energy differences

$$E_p(p) - E_0 = e(p > k_F), \quad (36)$$

$$E_0 - E_h(q) = e(q < k_F) \quad (37)$$

give the single-particle energy to create a quasiparticle and a quasihole, respectively. The energy per particle obtained by either adding or removing particles having  $k = k_F$  is

$$e(k_F) = \frac{E_0(\rho)}{N} + \frac{\rho}{N} \frac{\partial}{\partial \rho} E_0(\rho). \quad (38)$$

For a Fermi disk filled up to  $|\vec{k}| \leq k_F$  the ground state energy of the system is only kinetic given by  $E_0(\rho) = \frac{1}{2} \epsilon_F N$ , where  $\epsilon_F = (\hbar^2/2m)(4\pi/g_s)\rho$ . We are dealing with the fully spin polarized (spinless) case, so  $g_s$  is 1.

It is convenient to calculate the quasiparticle and quasihole excitation energies  $e(p > k_F)$  and  $e(q < k_F)$  by removing a small fraction  $x \ll 1$  of particles<sup>11</sup> ( $xN$  is number of removed fermions) from a thin ring at  $k = k_F$  ( $k = q$ ) in momentum space and putting them into a thin ring at  $k = p$  ( $k = k_F$ ) for the quasiparticle (quasihole) case.

Up to terms linear in  $x$  we have

$$E(x, k)/N = E_0/N + x[\pm e(k) \mp e(k_F)]. \quad (39)$$

The upper signs are for the quasiparticle case  $k = p > k_F$  and the lower signs for the quasihole case  $k = q < k_F$ .

The ‘‘mixed’’ density matrix for these occupations is a simple function of  $x$ ,  $k$ , and  $r_{12}$ :

$$l(x, k, r_{12}) = l(\vec{r}_1, \vec{r}_2) \pm x[J_0(kr_{12}) - J_0(k_F r_{12})]. \quad (40)$$

$E_0/N$  is the energy per particle of the system described by the wave function of Eq. (33), where no fermions have been removed from the Fermi disk, while  $E(x, k)/N$  is the energy per particle of our system when a small fraction  $x \ll 1$  of particles is removed from the Fermi disk and placed on a ring at wave vector  $k$  in momentum space. Both  $E(x, k)$  and  $E_0$  are calculated in the same way, by the FHNC method. Noting that  $E(x, k)/N = e(x, k)$ , and  $E_0/N = e_0$ , the quasiparticle energy is written

$$e_{qp}(q) = e(k) - e(k_F) = \frac{1}{x} [e(x, k) - e_0], \quad (41)$$

where  $q = k - k_F > 0$ . Then the effective mass  $m^*(k)$  is given by

$$\frac{m^*(k)}{m_e} = \frac{\hbar^2}{m_e} \frac{k}{\frac{\partial}{\partial q} e_{qp}(q)}, \quad (42)$$

where  $m_e$  is the bare electron mass.

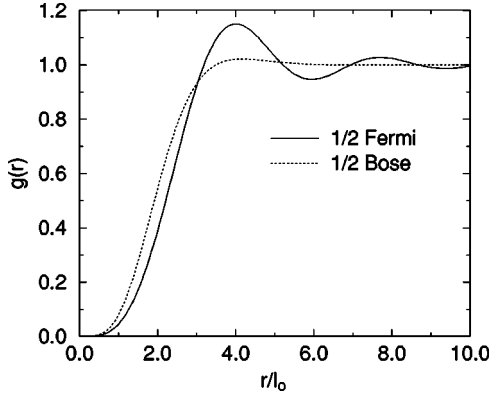


FIG. 1. Radial distribution function  $g(r)$  for the  $\nu=1/2$  state obtained from the unprojected Fermi wave function  $\Psi_{\nu=1/2}^{Fermi}$  and the projected Bose Laughlin-like wave function  $\Psi_{\nu=1/2}^{Bose}$ . Calculations were done neglecting the elementary diagrams, namely, within the FHNC/0 and HNC/0 approximations, respectively, for the Fermi and Bose cases.

## V. RESULTS

In the present work we applied the FHNC theory to the half-filled state of the FQHE, employing the unprojected Fermi half-filled wave function

$$\Psi_{\nu=1/2}^{Fermi} = \prod_{j < k}^N (z_j - z_k)^2 \text{Det}\{\varphi_{\vec{k}}(\vec{r})\} \quad (43)$$

and other unprojected wave functions that incorporate the physics of CF's at such filling. For the sake of simplicity, the elementary diagrams were neglected, so calculations were performed within the so-called FHNC/0 approximation.

For any given wave function  $\Psi_\nu$ , which describes a given state  $\nu$ , we calculated the radial distribution function  $g_\nu(r)$  and the interaction energy per particle was computed from

$$u_\nu = \frac{1}{N} \frac{\Psi_\nu | \hat{V} | \Psi_\nu}{\Psi_\nu | \Psi_\nu} = \frac{\rho_e}{2} \int d^2r [g_\nu(r) - 1] v(|\vec{r}|). \quad (44)$$

Except in the trivial case of  $\Psi_{\nu=1/2}^{Bose}$ , where the kinetic energy per particle is

$$\frac{1}{N} \frac{\Psi_{\nu=1/2}^{Bose} | \hat{K} | \Psi_{\nu=1/2}^{Bose}}{\Psi_{\nu=1/2}^{Bose} | \Psi_{\nu=1/2}^{Bose}} = \frac{1}{2} \hbar \omega_c, \quad (45)$$

its calculation is not easy at all to perform within the FHNC approach, so we devoted our interest mainly to the calculation of the interaction energy per particle.

In Fig. 1 we plot the radial distribution function  $g_{\nu=1/2}(r)$ , obtained from the unprojected  $\Psi_{\nu=1/2}^{Fermi}$  and  $\Psi_{\nu=1/2}^{Bose}$  wave functions. Its calculation in the Bose case was done by employing the Bose hypernetted-chain (HNC) method, which is rather standard and easier than the FHNC method. The ground state interaction energy per particle, obtained from the unprojected  $\Psi_{\nu=1/2}^{Fermi}$ , was found to be  $u_{\nu=1/2}^{Fermi} = -0.503(1/4\pi\epsilon_0)(e^2/\epsilon l_0)$ , a value rather lower than the value suggested from exact diagonalizations<sup>12</sup> of small systems of electrons.

The source of such discrepancy is the missing projection of  $\Psi_{\nu=1/2}^{Fermi}$  into the LLL. We performed a careful study of the

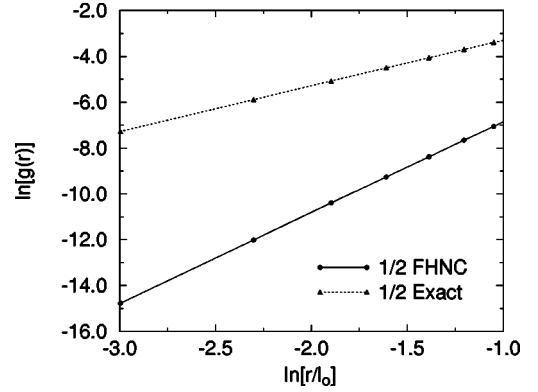


FIG. 2. Small- $r$  behavior of  $g_{\nu=1/2}^{Fermi}(r)$  on a logarithmic scale  $\ln[g(r)]$  versus  $\ln[r/l_0]$ . One observes that  $g_{\nu=1/2}^{Fermi}(r)$ , obtained from the unprojected Fermi wave function, has an erroneous  $g_{\nu=1/2}^{Fermi}(r) \sim (r/l_0)^4$  dependence instead of the correct  $(r/l_0)^2$  one of the projected case, suggested from exact numerical diagonalizations (Ref. 13).

small- $r$  behavior of the unprojected  $g_{\nu=1/2}^{Fermi}(r)$  for the case being. As shown in Fig. 2, we found that the radial distribution function has an erroneous  $g_{\nu=1/2}^{Fermi}(r) \sim (r/l_0)^4$  behavior instead of the  $(r/l_0)^2$  one suggested by exact numerical diagonalizations,<sup>13</sup> which of course do not suffer from the missing projection into the LLL. As a consequence, smaller values of the unprojected  $g_{\nu=1/2}^{Fermi}(r)$  at short  $r$  make the interaction energy per particle lower than the projected ones.

In the calculation of  $g_{\nu=1/2}^{CS}(r)$  corresponding to the CS wave function  $\Psi_{\nu=1/2}^{CS}(B^*) = \lim_{p \rightarrow \infty} \Psi_{\nu=p/(2p+1)}^{CS}(B^*)$ , where the unprojected  $\Psi_{\nu=p/(2p+1)}^{CS}(B^*)$  is given by

$$\Psi_{\nu=p/(2p+1)}^{CS}(B^*) = \prod_{j < k}^N \frac{(z_j - z_k)^2}{|z_j - z_k|} |\Phi_p(B^*)\rangle, \quad (46)$$

we observe that

$$|\Psi_{\nu=p/(2p+1)}^{CS}(B^*)|^2 = |\Phi_p(B^*)|^2, \quad (47)$$

which is just a squared determinant of single-particle eigenfunctions for  $p$  Landau levels, subjected to an effective magnetic field  $B^*$ , where  $p=1, 2, \dots$ . In this special case, the calculation of the interaction energy per particle  $u_{\nu=p/(2p+1)}^{CS}$  is exact because  $g_{\nu=p/(2p+1)}^{CS}(r)$  can be exactly computed within the FHNC framework.

In Table I we show the exact results for the interaction energy per particle  $u_{\nu=p/(2p+1)}^{CS}$  computed from the unprojected CS wave function of Eq. (46). In the fourth column we show the approximated variational Monte Carlo (VMC) results of Kamilla and Jain<sup>14</sup> for some of these states.

We stress again that our results are exact, without any approximation, so it seems that the above VMC treatment becomes less accurate for  $\nu \rightarrow 1/2$ . A reasonable extrapolation of these values for  $p \rightarrow \infty$  gives an estimate

$$u_{\nu=1/2}^{CS} = \lim_{p \rightarrow \infty} u_{\nu=p/(2p+1)}^{CS} \approx -0.425 \frac{1}{4\pi\epsilon_0} \frac{e^2}{\epsilon l_0}, \quad (48)$$

TABLE I. Interaction energies per particle  $u_\nu$ , expressed in units  $(1/4\pi\epsilon_0)(e^2/\epsilon l_0)$ , computed using the unprojected Chern-Simons wave function,  $\Psi_\nu^{CS}(B^*) = \prod_{j<k}^N [(z_j - z_k)^2 / |z_j - z_k|^2] \Phi_p(B^*)$  for fillings  $\nu = p/(2p+1)$ . The values in the third column refer to the FHNC/0 results, which in this case are exact, while in the fourth column we report the recent estimates of Kamilla and Jain (Ref. 14) obtained from a variational Monte Carlo simulation in the spherical geometry.

$\nu$	$p$	FHNC/0	Ref. 14
1/3	1	-0.361800	-0.3619(90)
2/5	2	-0.385343	-0.3848(16)
3/7	3	-0.395990	-0.3947(15)
4/9	4	-0.402064	-0.4007(16)
5/11	5	-0.405992	
6/13	6	-0.408742	
7/15	7	-0.410776	
8/17	8	-0.412341	
9/19	9	-0.413583	
10/21	10	-0.414592	

which is higher than the exact diagonalization results at  $\nu=1/2$ . In Fig. 3 we show the interaction energy per particle values  $u_{\nu=p/(2p+1)}^{CS}$  as a function of  $p=1,2,\dots$

The calculations employing the unprojected  $\Psi_\nu^{CF}(B)$  wave function are more difficult to perform, but the FHNC theory needed to describe them is not different from the previous cases. A detailed description is given elsewhere,<sup>15</sup> so we limit ourselves to the presentation of the results for the interaction energy values for the fillings  $\nu=p/(2p+1)$  given in Table II. An extrapolation of these values for  $\nu \rightarrow 1/2$  gives an estimate very close to the value for the  $\Psi_{\nu=1/2}^{Bose}$  case:

$$u_{\nu=1/2}^{CF} = \lim_{p \rightarrow \infty} u_{\nu=p/(2p+1)}^{CF} \approx -0.479(9) \frac{1}{4\pi\epsilon_0} \frac{e^2}{\epsilon l_0} \quad (49)$$

and similarly for  $g_{\nu=1/2}^{CF}(r)$ .

The radial distribution function  $g_{\nu=p/(2p+1)}^{CF}(r)$  obtained from the unprojected  $\Psi_{\nu=p/(2p+1)}^{CF}(B)$  does not seem to have

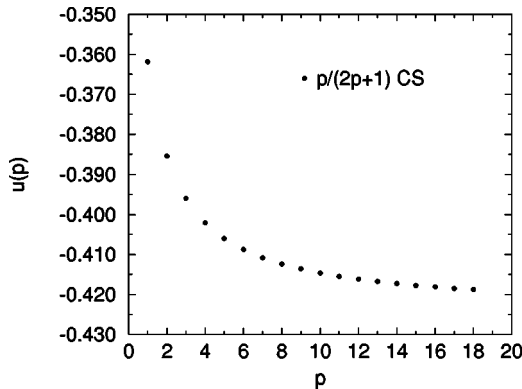


FIG. 3. Interaction energy per particle  $u_{\nu=p/(2p+1)}^{CS}$  for the unprojected Chern-Simons wave function  $\Psi_{\nu=p/(2p+1)}^{CS}(B^*)$  plotted as a function of the number of filled Landau levels  $p$ . The energies are expressed in the standard units  $(1/4\pi\epsilon_0)(e^2/\epsilon l_0)$ .

TABLE II. Interaction energies per particle  $u_\nu$ , expressed in units  $(1/4\pi\epsilon_0)(e^2/\epsilon l_0)$ , computed using the unprojected  $\Psi_{\nu=p/(2p+1)}^{CF}(B)$  wave function. The values in the second column refer to the FHNC/0 approximation, while in the third column we report the estimates of Jain and Kamilla (Ref. 17) obtained using projected CF wave functions in the spherical geometry.

$\nu$	(FHNC/0)	Ref. 17
1/3	-0.40257	-0.409828(27)
2/5	-0.43054	-0.432804(62)
3/7	-0.44510	-0.442281(62)
4/9	-0.45300	-0.447442(115)
5/11	-0.45796	-0.450797(175)
6/13	-0.46137	
7/15	-0.46386	
8/17	-0.46576	

visible Fermi-looking features. On the contrary, the radial distribution function obtained from the unprojected CF wave function

$$\Psi_{\nu=p/(2p+1)}^{CF}(B^*) = \prod_{j<k}^N (z_j - z_k)^2 |\Phi_p(B^*)\rangle, \quad (50)$$

where  $B^* = B 1/(2p+1)$  for  $\nu = p/(2p+1)$ , does have Friedel-looking oscillations, in agreement with the results by Kamilla *et al.*<sup>16</sup> We computed the radial distribution function at  $\nu=6/13$  corresponding to both wave functions  $\Psi_\nu^{CF}(B)$  and  $\Psi_\nu^{CF}(B^*)$  and the oscillations in the  $B^*$  case are evident from Fig. 4.

As our major interest was concentrated in the unprojected Fermi half filled wave function  $\Psi_{\nu=1/2}^{Fermi}$ , using the method described in Sec. IV, we computed the particle-hole excitation spectrum of this state by adopting a technique previously used in nuclear physics.<sup>11</sup> The supposedly low-energy Fermi excitations should have an effective mass  $m^*(k)$  determined by interelectron interactions only. Once we are able to calculate the interaction ground state energy per particle

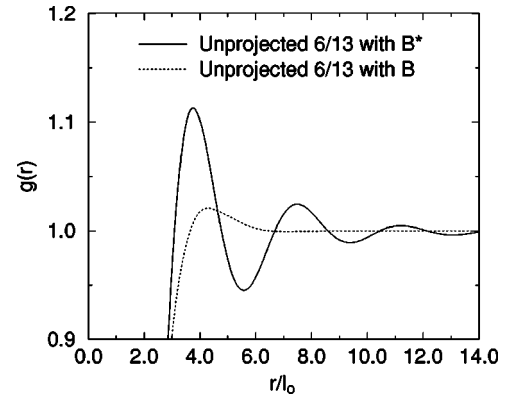


FIG. 4. For the fractional filling  $\nu=6/13$ , we show the radial distribution function  $g_\nu^{CF}(r)$  obtained from the unprojected  $\Psi_{\nu=6/13}^{CF}(B^*)$  (solid line) and the unprojected  $\Psi_{\nu=6/13}^{CF}(B)$  (dotted line). For  $\Psi_{\nu=6/13}^{CF}(B^*)$ , Friedel-like oscillations of  $g_\nu^{CF}(r) - 1$  are quite visible, in good agreement with the results of Kamilla *et al.* (Ref. 16).

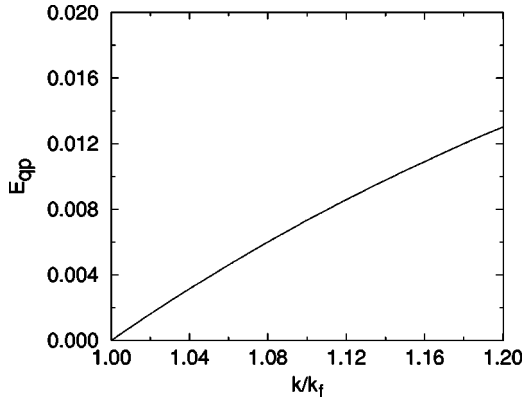


FIG. 5. Fermi quasiparticle excitation spectrum for the unprojected half-filled Fermi state  $\Psi_{\nu=1/2}^{Fermi}$ . The Fermi quasiparticle energy  $E_{qp}(q)$  computed from the interelectron correlations only and expressed in the units of  $(1/4\pi\epsilon_0)(e^2/\epsilon l_0)$  is given as a function of  $k/k_F$ , where  $q=k-k_F$  and  $k_F$  is the corresponding Fermi wave vector. For  $k/k_F \approx 1$  there is a linear dependence of  $E_{qp}(q)$  on  $q$ .

for several mixed  $\Psi_{\nu=1/2}^{Fermi}(\{\vec{r}_i\}, x)$  states, we are able to compute the quasiparticle and quasihole energies.

In Fig. 5 we plot the quasiparticle excitation spectrum  $e_{qp}(q)$  as a function of  $q=k-k_F > 0$ . It was found that in the long-wavelength limit ( $q \rightarrow 0$ ), the quasiparticle excitation energy expressed in units  $(1/4\pi\epsilon_0)(e^2/\epsilon l_0)$  is linearly proportional to  $q$  expressed in units  $1/l_0$  with  $\alpha=0.082$ . In these units

$$e_{qp}(q) = \alpha q. \quad (51)$$

From the above quasiparticle excitation spectrum, we compute the effective mass  $m^*(k)$  of the Fermi excitations by applying Eq. (42).

Using the dielectric constant  $\epsilon=12.6$  appropriate for GaAs and the magnetic field  $B=10$  T, taken from Halperin *et al.*,<sup>7</sup> we find with striking accuracy the result

$$m^*(k=k_F) = m_e, \quad (52)$$

in accordance with the mean field prediction of not imposing the LLL constraint. This indicates the high accuracy of the adapted method used to compute the Fermi excitation spectrum in a 2D problem, like the FQHE. Further, the urgent need of a LLL projection scheme incorporated to the FHNC theory is pointed out.

## VI. CONCLUSIONS

The Fermi hypernetted-chain theory was applied to the study the filling factor  $\nu=1/2$  of the fractional quantum Hall

effect. Calculations were done by neglecting the elementary diagrams on the cluster expansion of  $g_\nu(r)$ , namely, adopting the so-called FHNC/0 approximation. This technique, which has the priority to treat exactly in the thermodynamic limit the many-body correlated systems, was employed to study several unprojected wave functions used to describe this filling factor.

Our main interest was concentrated on an unprojected Fermi wave function  $\Psi_{\nu=1/2}^{Fermi}$ , but calculations were extended to other unprojected wave functions of the form  $\Psi_{\nu=p/(2p+1)}^{CS}$ ,  $\Psi_{\nu=p/(2p+1)}^{CF}(B)$ , and  $\Psi_{\nu=p/(2p+1)}^{CF}(B^*)$ , possible candidates to describe the  $\nu=1/2$  state as the limit  $p \rightarrow \infty$ . For the Fermi unprojected state  $\Psi_{\nu=1/2}^{Fermi}$  we studied both ground state and excited state properties, while several other ground state quantities such as the radial distribution function, structure factor, and interaction energy per particle were computed for the other wave functions.

The calculation of interaction energy per particle for the unprojected Chern-Simons wave function  $\Psi_{\nu=p/(2p+1)}^{CS}$  is exact within the FHNC approach and this is an important observation for future investigations. Among these unprojected wave functions,  $\Psi_{\nu=1/2}^{CF}(B)$  gives an estimate of the interaction energy and some other features, very similar to the  $\Psi_{\nu=1/2}^{Bose}$  case.

The radial distribution function obtained from  $\Psi_{\nu=p/(2p+1)}^{CF}(B)$  for  $p \gg 1$  does not have Fermi-looking features, while  $\Psi_{\nu=p/(2p+1)}^{CF}(B^*)$  and  $\Psi_{\nu=1/2}^{Fermi}$  do. After computing the Fermi quasiparticle/quasihole excitation spectrum for the unprojected  $\Psi_{\nu=1/2}^{Fermi}$  state, the resulting effective mass of the quasiparticles close to the Fermi surface  $k_F$  was found to be exactly the bare mass of the electrons, in agreement with the mean-field prediction of not imposing the LLL projection.

The accuracy of the method was tested to be high, so if a reasonable scheme to perform the LLL projection within the FHNC is found, then the calculation of the effective mass near the Fermi radius can be done accurately. Attempts in a such direction are in progress.

## ACKNOWLEDGMENTS

The authors thank Professor E. Tosatti for useful discussions and suggestions. This work was supported by European Community Contracts Nos. HCMCHRXCT94-0456, ERBCHRXCT-940438, and ERBCHRXCT-920062. Part of this work was carried out at the Ames Laboratory, which is operated for the U.S. Department of Energy by Iowa State University, and was supported by the Director for Energy Research, Office of Basic Energy Sciences of the U.S. Department of Energy.

<sup>1</sup>D. C. Tsui, H. L. Stormer, and A. C. Gossard, Phys. Rev. Lett. **48**, 1559 (1982).

<sup>2</sup>For a review see *The Quantum Hall Effect*, edited by R. E. Prange and S. M. Girvin (Springer-Verlag, New York, 1990); *The Fractional Quantum Hall Effect*, edited by T. Chakraborty and P. Pietiläinen (Springer-Verlag, New York, 1988).

<sup>3</sup>R. B. Laughlin, Phys. Rev. Lett. **50**, 1395 (1983)

<sup>4</sup>R. L. Willett, J. P. Eisenstein, H. L. Stormer, D. C. Tsui, A. C. Gossard, and J. H. English, Phys. Rev. Lett. **59**, 1776 (1987).

<sup>5</sup>R. L. Willett, M. A. Paalanen, R. R. Ruel, K. W. West, L. N. Pfeiffer, and D. J. Bishop, Phys. Rev. Lett. **65**, 112 (1990).

<sup>6</sup>F. D. M. Haldane, Phys. Rev. Lett. **55**, 2095 (1985).

- <sup>7</sup>B. I. Halperin, P. A. Lee, and N. Read, *Phys. Rev. B* **47**, 7312 (1993).
- <sup>8</sup>J. K. Jain, *Phys. Rev. Lett.* **63**, 199 (1989).
- <sup>9</sup>A. Lopez and E. Fradkin, *Phys. Rev. B* **44**, 5246 (1991).
- <sup>10</sup>S. Fantoni and S. Rosati, *Lett. Nuovo Cimento* **10**, 545 (1974); *Nuovo Cimento A* **25**, 593 (1975).
- <sup>11</sup>B. Friedman and V. R. Pandharipande, *Phys. Lett.* **100B**, 3 (1981).
- <sup>12</sup>G. Fano, F. Ortolani, and E. Tosatti, *Nuovo Cimento D* **9**, 1337 (1987).
- <sup>13</sup>D. Yoshioka, *Phys. Rev. B* **29**, 6833 (1984).
- <sup>14</sup>R. K. Kamilla and J. K. Jain, *Phys. Rev. B* **55**, 9824 (1997).
- <sup>15</sup>O. Ciftja and S. Fantoni, *Phys. Rev. B* **56**, 13 290 (1997).
- <sup>16</sup>R. K. Kamilla, J. K. Jain, and S. M. Girvin, *Phys. Rev. B* **56**, 12 411 (1997).
- <sup>17</sup>J. K. Jain and R. K. Kamilla, *Phys. Rev. B* **55**, R4895 (1997).